PROCEEDINGS of the
23rd International Congress on Acoustics

9 to 13 September 2019 in Aachen, Germany

Experimental Modelling of Tyre/Road Noise from Road Texture Spectra on Rubberized Road Surfaces

Alessandro DEL PIZZO[1]; Gonzalo DE LEÓN[1]; Luca TETI[2]; Francesco BIANCO[2], Antonino MORO[3], Luca FREDIANELLI[1], Gaetano LICITRA[1]

[1] Università di Pisa, Dipartimento di Fisica, Italy

[2] iPOOL srl, Italy

[3] IPCF-CNR, Italy

ABSTRACT

Road traffic noise is one of the most common sources of acoustic pollution in urbanized environments and, therefore, its mitigation is fundamental for urban planning. Since tyre/road interaction represents the main contribution to overall road traffic noise, the use of low noise road surfaces represents a useful way for reducing the acoustic impact of road traffic, acting on the main generation mechanism of noise. In this work, both acoustic performances and road texture of several low noise rubberized surfaces and conventional road surfaces were measured and compared. In particular, acoustic performances were monitored using the CPX method, while road texture measurements were performed using a laser triangulation sensor. Road profiles were processed with a tyre envelopment algorithm called indenter method and the spectra of the resulting signal was compared with the CPX spectra on each road surface. Findings show that surfaces with crumb rubber within the mixture behave differently compared to conventional surfaces at high frequency, while noise at frequencies lower than 1 kHz seems unaffected by the presence of crumb rubber.

Keywords: Rubberized Surfaces, Road Texture, CPX Measurements

1.1 INTRODUCTION

Road traffic noise in urban areas represents the most common sourc of noisee, as reported in several works, such as the 2002 European Environmental Noise Directive (END) and its revision (1) and, therefore, the study of its generation mechanisms is of paramount importance for the proposal of suitable mitigation actions.

Road traffic noise is caused by three different generation mechanisms: noise produced by the power unit, aerodynamic noise induced by the car motion at high speed and, finally, tyre/road interaction. For light vehicles, engine noise is dominant at speeds lower than 35 km/h and profile aerodynamics becomes relevant only at speeds higher than the typical motorway speed (i.e. 130 km/h), tyre/road noise is the dominant source from 35 to 130 km/h (2).

Tyre/road noise itself is due to both airborne and structure-borne contributions (4). The former causes high frequency noise produced by the compression and subsequent expansion of the air trapped within the tyre/road interface, while the latter is caused by tyre vibrations and is dominant at frequencies below 1 kHz. In particular, the fundamental properties of road surfaces that play a role in sound generation mechanisms are the surface macro and megatexture, defined by ISO 13473-2, porosity and layer thickness (5).

In this paper, the relationship between road texture and tyre/road noise was analysed from an experimental point of view, monitoring the acoustic performances of the surfaces using the CPX method defined by ISO 11819-2:2017 and road texture on conventional and rubberized surfaces and evaluating the correlation coefficient and linear regression coefficients between one-third octave bands of CPX noise and road texture. A test based on t-statistics, performed on the slopes found for conventional and rubberized pavements, was then used to distinguish regions where the surfaces showed a different relation between tyre/road noise and road texture.

1 alessandro.delpizzo@df.unipi.it

An algorithm based on the works of Goubert and Sandberg (6) was also used, in order to take into account only the part of road texture actually into contact with the tyre.

2.1 STATE OF ART

Noise reduction at the source is a very cost effective treatment (7) and, therefore, many European studies have focused their attention on low noise surfaces, such as porous asphalts, SMA, thin, very thin and ultra-thin surfacing and surfaces that include rubber in their mix. In particular, more and more attention is paid to pavements which include crumb rubber deriving from end-of-life tyres. In this way, noise reduction goes hand-in-hand with the concepts of green and circular economy.

The main kinds of surfaces which include rubber are poro elastic road surfaces (PERS) and rubberized surfaces. While the former uses rubber as a main component of the mix (7), rubberized road surfaces are built using hot asphalt mixes containing crumb rubber which acts as a modifier, in order to improve the acoustical properties of the binder (8). Rubberized surfaces are subdivided in two categories, according to their production means: *wet* road surfaces are created by blending crumb rubber with liquid asphalt cement (AC) before mixing AC with the aggregate, while in the *dry* process, crumb rubber is added to the hot aggregate (8).

The acoustical properties of these surfaces have been monitored by several studies (9, 10), with specific projects launched to evaluate their effectiveness (10), showing that rubberized surfaces produce lower noise emissions compared to DAC of the same age.

Since, as already stated, the main source of road traffic noise is represented by tyre/road noise, the study of road and tyre properties is fundamental.

Among several road surface properties, road texture covers an important role in noise generation (2, 3, 11). It is defined as the deviation of a pavement surface from a true planar surface, caused by the random disposition of the surface elements and their superficial roughness (12). The study of road texture is usually performed using spectral analysis in constant-percentage bandwidth, by means of octave or one-third octave bands. It is also customary to report texture spectra using texture levels, as defined by ISO 13473-4.

Based on the different wavelengths of the road profile signal, road texture is divided in three regions: microtexture includes wavelengths shorter than 0.5 mm, wavelengths that range from 0.5 mm to 50 mm are addressed as macrotexture while longer wavelengths, up to 500 mm, are called megatexture. Longer wavelenghts are addressed as unnevenness.

While microtexture is caused by roughness of the visible surface elements and, therefore, it depends on the nature of the stones and chippings used, macrotexture is due to the shape, dimension and positioning of the aggregates. Bumps and ripples present on road surfaces cause the presence of megatexture.

Previous studies (12, 13) underline the positive influence of high texture levels at wavelengths shorter than 10 mm on the mitigation of tyre/road noise, since it reduces air compression due to the tyre tread, while texture levels around 63 mm play a key role in the generation of structure-borne noise, since it induces tyre vibrations. Positive texture, produced by a surface characterised by high peaks, results more aggressive than a surface crossed by deep valleys and grooves from an acoustic point of view, since the peaks induce vibrations of the tyre walls (13). However, an abrupt spectral analysis of the profile signal cannot distinguish between positive and negative texture and, therefore, tyre envelopment algorithms have been developed, in order to calculate the road texture actually into contact with the tyre. In this work, the indenter algorithm developed by Goubert and Sandberg (6) was used. This study showed that the tyre envelopment follows the road profile until a certain depth dependent on the kind of tyre and the speed of the vehicle.

3.1 Methods and Sites Analysed

Noise and road texture measurements were carried out during Novemeber 2017 on 17 sites on the highway that connects Merano to Bolzano, in the region of Trentino-Alto Adige/Südtirol in Northern Italy. Since the maximum distance between sites is about 20 km and the difference in height at the starting and ending point of the highway is about 100 m, it is safe to assume that the sites are exposed to the same weather and traffic condition, minimising acoustic ageing influence on measurements (14).

Among the road surfaces, 7 were conventional dense surfaces, while the other 10 were rubberized

surfaces, equally subdivided in *dry* and *wet*, according to their means of production.

The mean grading curves of the dry, wet and reference surfaces are reported in Figure 1.

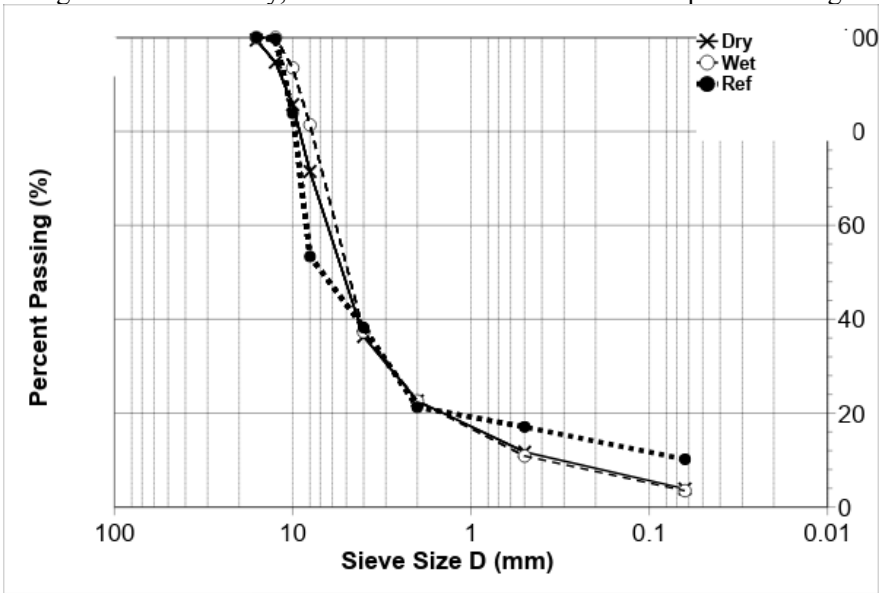

Figure 1 – Mean grading curves for the three kinds of road surfaces used

CPX and road texture measurements were compared, performing a linear regression between each couple of CPX and texture one-third octave bands, separately for rubberized and conventional road surfaces. After evaluating goodness-of-fit, a parallelism test based on the t-statistics was used. The results of of this test allow to discern regions where the slope that relates road texture to CPX noise does not change between the two kinds of surfaces from regions where statistically significant differences were found.

The flowchart and experimental plan of the work is presented in Figure 2.

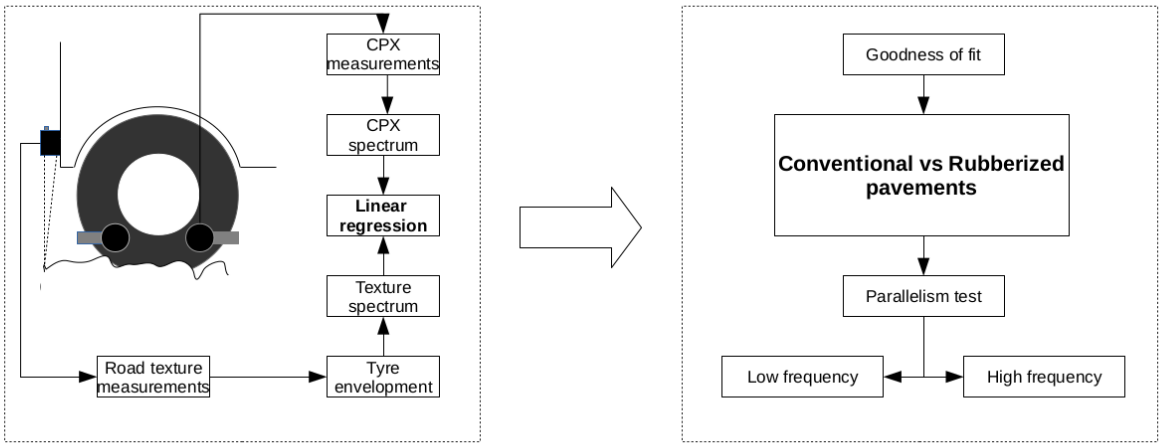

Figure 2 – Flowchart and experimental plan of the paper.

3.1 The CPX method

The CPX method (15) aims to evaluate tyre/road noise close to the source. The protocol adopted is based on a modified procedure (16) with changes regarding post-processing.

In order to comply with the last version of ISO 11819-2 (15), the Standard Reference Test Tyre (SRTT) was used and normalisations for temperature and tyre hardness were performed at 22 °C and 66 Shore A. Moreover, due to the logarithmic dependence between vehicle speed and tyre/road

noise, a reference speed is required: the nature of the roads under investigation led to the choice of a reference speed equal to 100 km/h.

The correction for temperature and hardness has been applied to the one-third band levels, despite it is strictly valid for broadband levels, due to the current lack of studies on this topic.

During the measurement sessions, several acquisitions on the same surface were performed at different speeds. In the post-processing phase, the site is subdivided in segments and a minimum χ^2 iterative algorithm was used in each segment for fitting sound levels with speed, in order to compute the one-third octave bands spectrum at the reference speed. Finally, the mean value of the sound pressure level within each band is used to characterise the whole site.

The main modification to the official protocol regards data analysis, since the test sites were divided in segments 6.18 m long, i.e. three times a tyre circumference, instead of using the standard section length of 20 m, in order to increase the spatial resolution of the analysis.

For each surface, the mean CPX spectrum and related uncertainty were then calculated.

3.2 Road texture measurements

All texture measurements were carried out simultaneously with CPX measurements. The experimental setup is based on a triangulation sensor, a piezoelectric accelerometer and a rotary encoder (12, 17), whose outputs are combined in order to yield the road profile, with a horizontal sampling length equal to 0.5 mm.

The road profile was then processed using the indenter algorithm developed by Goubert and Sandberg, in order to simulate tyre deformation caused by the profile itself. The algorithm is based on experimental measures of SRTT deformation on known profiles and therefore represents the ideal solution for this study, since it is based on the same tyre adopted for the measurements.

The profile obtained after the tyre envelopment was then divided in segments and fitted with an autoregressive model based on the Yule-Walker method, in order to reduce signal noise. Then, the one-third octave spectra were derived following the prescriptions of the fourth method reported in ISO/TS 13473-4:2008.

3.3 Measurement uncertainties

The three sources of uncertainty related to mean CPX values are due to the fitting process in each segment, data dispersion around the mean value and:

> several factors and processes, whose cause and nature of disturbance are either known, but randomly distributed in an uncontrollable way, or are of a systematic nature, but affect the result in an unpredictable way (15).

The first source is assumed to be equal to the uncertainty of the measurement process within each segment, while the second source is taken into account by evaluating the standard deviation of data and describes the spatial homogeneity of the installation. The last factor, instead, was neglected in this analysis since the conditions of measurements do not vary greatly within the different sessions.

An estimate of measurement uncertainties for texture spectra within a segment is derived using the same procedure adopted in (17), with the quadratic sum of two components. The first component takes into account data dispersion around the mean value and is equal to the standard deviation of each band for each site, while the second contribution is inversely proportional to the root of the bandwidth of each band times the length of each section and is assumed to be the uncertainty of the texture measurement process.

4.1 ANALYSIS AND RESULTS

4.1 Correlation and linear regression

In order to perform a qualitative evaluation, the correlation coefficient between each couple of enveloped road texture and CPX noise bands was calculated.

The correlation curves, shown in Figure 3 (left) and (right) separately for rubberized and conventional road surfaces, are in accordance with previous studies, which highlight a positively correlated low frequency noise and a high frequency zone negatively correlated.

However, road surfaces with crumb rubber added in their mix are present a larger region in which negative correlation occurs. Conversely, the positively correlated zone occupies a smaller frequency region for rubberized surfaces, compared to the conventional ones.

This difference could represent a first acoustical benefit of using rubberized surfaces, since the region that contributes positively to noise emission is significantly reduced.

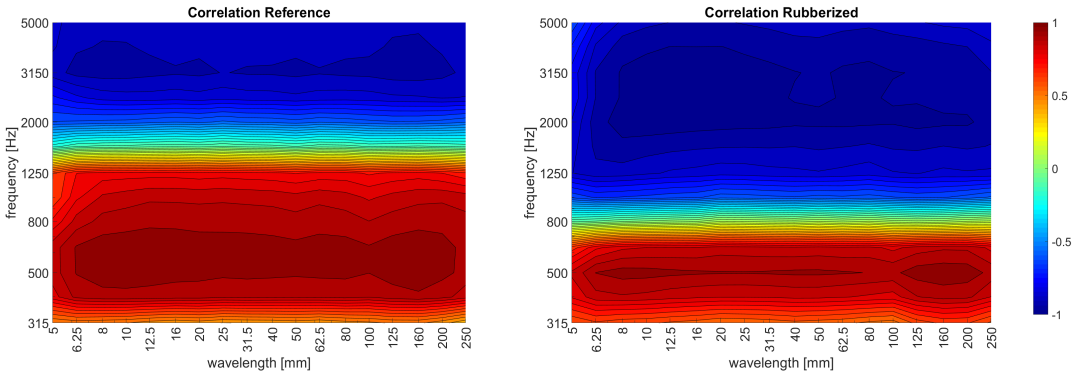

Figure 3 – correlation coefficient for the conventional reference surfaces (left). Correlation coefficient for rubberized surfaces (right).

Linear regressions were performed for each couple of bands of enveloped road texture and CPX noise and the parallelism test based on t-statistics took into account only regressions that showed a r^2_{adj} value greater than 0.7, chosen as a threshold to identify high goodness-of-fit.

The values of the r^2_{adj} calculated for each regression are reported in Figure 4 and 5. As expected, high r^2_{adj} values were found where strong correlation is present.

Adjusted r^2 for Reference Surfaces

Frequency [Hz] \ Wavelength [mm]	250	200	160	125	100	80	62.5	50	40	31.5	25	20	16	12.5	10	8	6.25	5
5000	0.67	0.71	0.74	0.74	0.71	0.70	0.68	0.71	0.69	0.69	0.67	0.70	0.68	0.70	0.72	0.73	0.70	0.61
4000	0.47	0.60	0.67	0.67	0.62	0.61	0.58	0.60	0.59	0.58	0.57	0.61	0.58	0.60	0.65	0.65	0.61	0.47
3150	0.74	0.79	0.81	0.82	0.80	0.79	0.77	0.79	0.77	0.77	0.75	0.78	0.77	0.79	0.81	0.82	0.80	0.69
2500	0.79	0.80	0.79	0.78	0.77	0.77	0.77	0.79	0.77	0.77	0.76	0.77	0.76	0.77	0.77	0.76	0.71	0.58
2000	0.53	0.57	0.59	0.60	0.60	0.57	0.55	0.58	0.56	0.55	0.54	0.57	0.55	0.56	0.59	0.61	0.64	0.62
1600	-0.06	-0.04	-0.03	-0.03	-0.05	-0.06	-0.06	-0.05	-0.06	-0.06	-0.08	-0.05	-0.06	-0.04	-0.03	-0.02	-0.01	0.00
1250	0.67	0.72	0.74	0.73	0.71	0.74	0.74	0.71	0.73	0.74	0.75	0.74	0.75	0.75	0.74	0.74	0.70	0.58
1000	0.84	0.85	0.85	0.82	0.79	0.83	0.85	0.82	0.84	0.85	0.85	0.85	0.86	0.86	0.83	0.82	0.72	0.53
800	0.89	0.91	0.96	0.94	0.81	0.85	0.88	0.86	0.87	0.88	0.88	0.87	0.88	0.88	0.85	0.83	0.75	0.59
615	0.76	0.88	0.94	0.92	0.83	0.86	0.85	0.85	0.86	0.86	0.85	0.87	0.88	0.89	0.90	0.89	0.80	0.57
500	0.74	0.85	0.90	0.87	0.79	0.84	0.84	0.82	0.83	0.84	0.83	0.85	0.86	0.88	0.88	0.88	0.77	0.52
400	0.66	0.77	0.83	0.80	0.73	0.77	0.76	0.75	0.76	0.77	0.76	0.78	0.79	0.81	0.82	0.81	0.76	0.55
315	-0.03	0.01	0.05	0.05	0.02	0.01	0.00	0.01	0.00	0.00	0.00	0.01	0.00	0.02	0.04	0.05	0.06	0.04

Figure 4 – r^2_{adj} for the conventional reference surfaces. Values of r^2_{adj} higher than 0.7 are highlighted in red.

Adjusted r^2 for Rubberized Surfaces

Frequency [Hz] \ Wavelength [mm]	250	200	160	125	100	80	62.5	50	40	31.5	25	20	16	12.5	10	8	6.25	5
5000	0.74	0.81	0.80	0.81	0.88	0.85	0.88	0.82	0.91	0.85	0.86	0.88	0.87	0.87	0.84	0.79	0.72	0.52
4000	0.77	0.91	0.92	0.96	0.86	0.91	0.90	0.88	0.89	0.90	0.91	0.92	0.94	0.93	0.94	0.88	0.75	0.51
3150	0.80	0.90	0.89	0.91	0.88	0.91	0.91	0.89	0.91	0.91	0.93	0.93	0.97	0.97	0.98	0.91	0.81	0.52
2500	0.80	0.91	0.88	0.90	0.89	0.89	0.90	0.88	0.91	0.91	0.92	0.93	0.98	0.97	0.96	0.92	0.80	0.78
2000	0.80	0.95	0.92	0.98	0.88	0.89	0.96	0.89	0.89	0.94	0.91	0.93	0.94	0.94	0.98	0.94	0.83	0.59
1600	0.68	0.68	0.67	0.71	0.70	0.65	0.68	0.68	0.64	0.69	0.69	0.69	0.71	0.74	0.76	0.79	0.72	0.51
1250	0.51	0.49	0.48	0.50	0.50	0.44	0.48	0.50	0.48	0.47	0.44	0.45	0.48	0.50	0.54	0.59	0.63	0.54
1000	0.15	0.19	0.22	0.22	0.21	0.17	0.18	0.18	0.19	0.18	0.16	0.16	0.20	0.21	0.23	0.25	0.27	0.23
800	-0.11	-0.11	-0.11	-0.11	-0.11	-0.10	-0.11	-0.11	-0.11	-0.11	-0.10	-0.10	-0.11	-0.11	-0.12	-0.12	-0.12	-0.12
615	0.38	0.50	0.68	0.44	0.34	0.43	0.41	0.42	0.37	0.41	0.41	0.44	0.44	0.46	0.40	0.37	0.29	0.14
500	0.62	0.92	0.95	0.92	0.75	0.83	0.83	0.84	0.85	0.83	0.82	0.81	0.75	0.69	0.77	0.83	0.73	0.48
400	0.54	0.66	0.72	0.64	0.47	0.51	0.54	0.55	0.56	0.54	0.53	0.54	0.57	0.60	0.63	0.63	0.63	0.43
315	0.12	0.19	0.21	0.16	0.07	0.07	0.10	0.11	0.12	0.11	0.10	0.10	0.13	0.15	0.17	0.18	0.20	0.16

Figure 5 – r^2_{adj} for the rubberized surfaces. Values of r^2_{adj} higher than 0.7 are highlighted in red.

4.2 Parallelism test

The parallelism test performed was based on a t-test on the regression coefficients, using the following equation:

$$t_{score} = \frac{b_1 - b_2}{SE_{(b_1 - b_2)}} \tag{1}$$

where b_1 is the slope of the regression for the rubberized surfaces and b_2 is the slope of the regression for the reference surfaces and $SE_{(b_1 - b_2)}$ is the standard error of the difference of the two angular coefficients. The values provided by Equation (1) were then used to test the hypothesis:

$$\begin{aligned} H_0 &: b_1 = b_2 \\ H_1 &: b_1 \neq b_2 \end{aligned} \tag{2}$$

comparing each t_{score} with the critical value $t_{crit}(0.975) = 2.16$ for $(n_1\text{-}2+n_2\text{-}2) = 13$ degrees of freedom, where n_1=10 is the number of rubberized surfaces and n_2 = 7 is the reference surface sample size.

Results identify two different regions, at 500 Hz and at 2.5 kHz, with opposite behaviour: at 500 Hz the slope coefficients of the two samples show no difference, while at 2.5 kHz statistically significant differences arise. A reduced matrix of the t-scores obtained is reported in Figure 6.

It is useful to remind that rolling noise at frequencies lower than 1 kHz is related to tyre vibration mechanisms, while noise at higher frequencies is due to airborne processes, not directly related to tyre perturbations. Bearing this in mind, it appears therefore that crumb rubber in the pavement mix does not influence tyre vibrations due to the impact of the tyre tread against the road asperities, while airborne noise, caused by the compression of air trapped between the tyre/road interface, is significantly influence by its presence.

In particular, the negative slope at 2.5 kHz results significantly increased on rubberized surfaces, as it can be inferred by observing Figure 7 (left) and (right).

Interestingly, no differences were found between the *wet* and *dry* processes.

t_{score} Values for zones with $r^2 > 0.7$ in both regressions

Frequency [Hz] \ Wavelength [mm]	5	6.25	8	10	12.5	16	20	25	31.5	40	50	62.5	80	100	125	160	200	250
5000	-	-0.28	-0.79	-1.04	-1.19	-	-	-	-	-	-1.65	-	-	-1.53	-1.57	-1.58	-1.77	-
4000	-	-	-	-	-	-	-	-	-	-	-	-	-	-	-	-	-	-
3150	-	-1.24	-1.79	-1.97	-2.10	-2.19	-2.56	-2.55	-2.70	-2.76	-2.78	-2.75	-2.88	-2.86	-2.72	-2.72	-2.95	-2.94
2500	-	-2.09	-2.67	-2.92	-3.04	-3.19	-3.47	-3.56	-3.65	-3.70	-3.67	-3.67	-3.88	-3.80	-3.69	-3.66	-3.83	-3.66
2000	-	-	-	-	-	-	-	-	-	-	-	-	-	-	-	-	-	-
1600	-	-	-	-	-	-	-	-	-	-	-	-	-	-	-	-	-	-
1250	-	-	-	-	-	-	-	-	-	-	-	-	-	-	-	-	-	-
1000	-	-	-	-	-	-	-	-	-	-	-	-	-	-	-	-	-	-
800	-	-	-	-	-	-	-	-	-	-	-	-	-	-	-	-	-	-
615	-	-	-	-	-	-	-	-	-	-	-	-	-	-	-	-	-	-
500	-	-1.08	-0.62	-0.35	-	0.28	0.76	0.95	1.09	1.04	1.25	1.17	1.47	1.36	0.93	0.85	0.97	-
400	-	-	-	-	-	-	-	-	-	-	-	-	-	-	-	0.38	-	-
315	-	-	-	-	-	-	-	-	-	-	-	-	-	-	-	-	-	-

Figure 6 – t_{score} matrix resulting from the parallelism test. Blue cells highlight differences, while red identifies cells where no statistical difference was found.

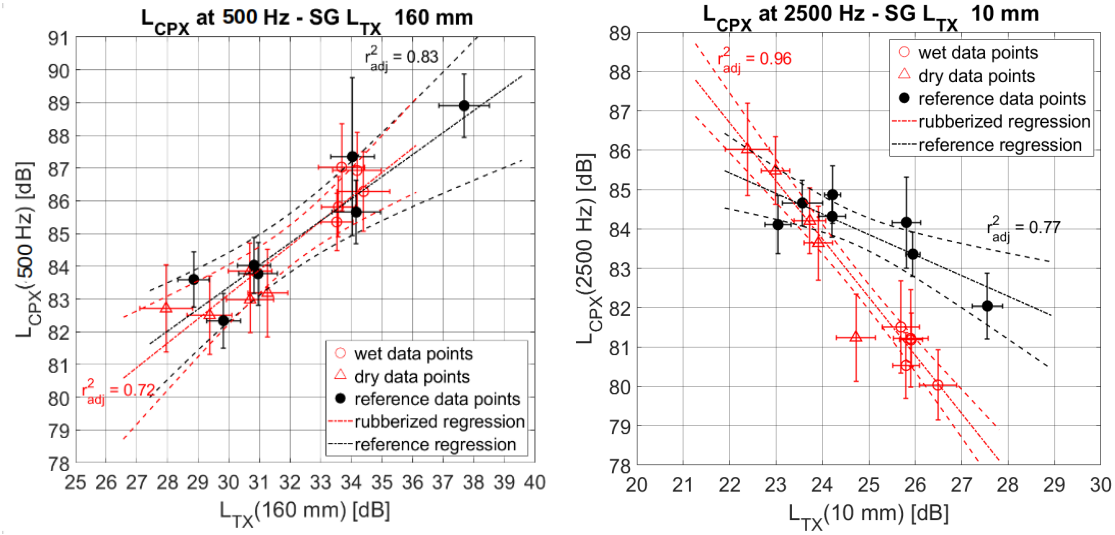

Figure 7 – Low frequency (500 Hz) as a function of enveloped texture levels (left). High frequency (2.5 kHz) as a function of enveloped texture levels at 10 mm (right).

5.1 CONCLUSIONS

Rubberized asphalts represent one of the most common mitigation actions for roads with high and continuous traffic flow, managing to blend the modern concept of green and circular economy with the necessity of improving the acoustical properties of road surfaces.

This work studied the variation of the interaction between road texture and tyre/road noise due to the presence of crumb rubber from end-of-life tyres in the road pavement mix. A novel tyre envelopment algorithm was also used, in order to take into account only the part of road texture in contact with the tyre.

The study was carried out by analysing the correlation between road texture and CPX noise levels in one-third octave bands and by performing linear regressions between each couple of CPX and road texture bands.

Results indicate that rubberized pavements show a greater frequency region negatively correlated with road texture compared to conventional surfaces.

A statistical test based on t-statistics was used to infer eventual differences between the linear regressions that showed a r^2_{adj} higher than 0.7 for both kinds of surfaces, with the identification of

two different regions, centred at 500 Hz and at 2.5 kHz. The 500 Hz band does not show statistical differences between conventional and rubberized surfaces, while the 2.5 kHz band shows a higher negative slope, highlighting a greater noise reduction potential of rubberized pavements compared to the conventional road surfaces.

This work, therefore, sheds new light on the effects of the use of crumb rubber in the road mix from an acoustic point of view. Further developments could include a physical model in oder to describe the role of crumb rubber in road traffic noise generation. An increase of the sample size would represent a significant improvement to the study, in order to confirm the relations found.

REFERENCES

1. European Commission. Report from the Commission to the European Parliament and the Council on the Implementation of the Environmental Noise Directive in accordance with Article 11 of Directive 2002/49/EC. COM/2017/015.
2. Sandberg U, Ejsmont J. Tyre/road noise reference book. Kisa, Sweden: INFORMEX; 2002.
3. Kuijpers, A., Van Blokland, G. Tyre/road noise models in the last two decades: a critical evaluation. Proc. INTER-NOISE and NOISE-CON Congress and Conference No. 2; 27-30 August 2001; The Hague, The Netherlands 2001. p. 2494-2499.
4. Morgan, P. A., Phillips, S. M., Watts, G. R. The localisation, quantification and propagation of noise from a rolling tyre. TRL Limited, 2007.
5. Praticò, F. G., Anfosso-Lédée, F. Trends and issues in mitigating traffic noise through quiet pavements. Procedia-Social and Behavioral Sciences 2012;53:203-212.
6. Goubert, L., Sandberg, U. Enveloping texture profiles for better modelling of the rolling resistance and acoustic qualities of road pavements. Symposium on Pavement Surface Characteristics (SURF), 8th; 2-4 May 2018, Brisbane, Australia 2018.
7. Sandberg, U., Kalman, B., Nilsson, R. Design guidelines for construction and maintenance of poroelastic road surfaces. Silvia Project Report Silvia-Vti-005-02-Wp4-141005; 2005.
8. Shatnawi, S. Comparisons of Rubberized Asphalt Binder: Asphalt-Rubber and Terminal Blend. Proc. Asphalt Rubber; 23-26 October 2012; Munich, Germany 2012.
9. Licitra, G., Cerchiai, M., Teti, L., Ascari, E., Fredianelli, L. Durability and variability of the acoustical performance of rubberized road surfaces. Appl Acoust. 2015;94:20-28.
10. Licitra, G., Cerchiai, M., Teti, L., Ascari, E., Bianco, F., Chetoni, M. Performance assessment of low-noise road surfaces in the Leopoldo project: comparison and validation of different measurement methods. Coatings 2015;5(1):3-25.
11. ISO 13473-2:2002 Characterization of pavement texture by use of surface profiles - Part 2: Terminology and basic requirements related to pavement texture profile analysis.
12. Del Pizzo, A., Teti, L., Bianco, F., Moro, A., Licitra, G. Influence of Texture on Tyre Road Noise Spectra in Rubberized Pavements. Manuscript submitted for publication to Appl Acoust. 2019.
13. Hamet, J. F., Klein, P. Road texture and tire noise. Proc. INTER-NOISE 2000; 27-30 August 2000; Nice, France 2000. p. 178-183.
14. Licitra, G., Moro, A., Teti, L., Del Pizzo, A., Bianco, F. Modelling of acoustic ageing of rubberized pavements. Applied Acoustics, 2019;146:237-245.
15. ISO 11819-2:2017 Acoustics -- Measurement of the influence of road surfaces on traffic noise -- Part 2: The close-proximity method.
16. Licitra, G., Teti, L., Cerchiai, M. A modified Close Proximity method to evaluate the time trends of road pavements acoustical performances. Applied Acoustics 2014;76:169-179
17. Del Pizzo, A., Bianco, F., Teti, L., Moro, A., Licitra, G. A New Approach for the Evaluation of the Relationship between Road Texture and Rolling Noise. Proc. of ICSV25, 8-12 July 2018; Hiroshima, Japan.